

## Wideband Bandpass Filter With Extremely Wide Upper Stopband — [Source link](#)

J.A.G. Malherbe

**Institutions:** University of Pretoria

**Published on:** 20 Apr 2018 - IEEE Transactions on Microwave Theory and Techniques (IEEE)

**Topics:** Chebyshev filter, Band-pass filter, Filter design, Stopband and Passband

Related papers:

- [Analysis and design of wideband bandpass filters with improved upper stopband](#)
- [An Optimum Ultra-Wideband \(UWB\) Bandpass Filter with Spurious Response Suppression](#)
- [Compact wide-passband and wide-stopband microstrip bandpass filter using multi-stub resonator](#)
- [Wideband bandpass filter using parallel-coupled line and step-impedance open stubs](#)
- [Compact differential ultra-wideband bandpass filter based on transversal filter concepts](#)

Share this paper:    

View more about this paper here: <https://typeset.io/papers/wideband-bandpass-filter-with-extremely-wide-upper-stopband-528h3x4tmm>

# Wideband Bandpass Filter with Extremely Wide Upper Stopband

J.A.G. Malherbe, *Life Fellow, IEEE*

**Abstract**— The realization of planar wideband bandpass filters with an extremely wide upper stopband, is described. The filter design differs from conventional approaches in that it is based on the choice of a wideband bandstop filter, to which a number of shunt shorted stubs are connected at specific nodes; the stubs provide transmission zeros at the origin. Two examples of wideband bandpass filters with extremely wide upper stopbands are presented: filters based on a 5<sup>th</sup> order Chebyshev wideband bandstop filter, and a pseudo-elliptic function ultra wideband bandstop filter. Relative passbands in excess of 100% are achieved, while the equivalent of at least four harmonic passbands is suppressed.

**Index Terms**— Ultra wideband, bandpass, wide upper stopband.

## I. INTRODUCTION

In many applications of transmission line bandpass filters, the existence of harmonic responses of passbands are problematic, and a large number of different approaches by which such responses are suppressed, have been proposed. In the case of narrow band bandpass filters, various methods include the employment of defected ground plane structures (DGS) [1], corrugated microstrip lines [2], pre-defined upper stopband characteristics [3], with folded stubs to extend the upper stopband [4], and the introduction of transmission zeros to suppress the upper stopbands [5]. Stub-loaded multimode resonators have been employed in the design of a bandpass filter with enlarged stopband [6]. Interdigital lines and spurlines generally yield wider bandwidths, and harmonic responses are suppressed by DGSs [7], [8]. Various configurations of ring resonators, together with stubs are also employed [9] – [14].

The design of a wideband bandpass filter, cascaded with a lowpass or pseudo-lowpass filter to remove harmonic responses has the disadvantage of increased size, while spurious responses limit the useful stop bandwidth [15] – [17].

The integrated connection of a bandpass filter and a lowpass structure eliminates the problem of size. A pseudo-lowpass structure has been integrated into a bandpass filter [18], effectively suppressing the harmonic responses of the bandpass structure. However, the spectrum of eliminated

harmonic responses is limited, as the two structures are not harmonically related, i.e. the resonant frequencies of the bandpass and lowpass filters are not harmonic multiples. This causes severe spurious spikes at frequencies well beyond the initial cutoff frequency of the lowpass filter, thus limiting the useful separation between the wanted passband and any unwanted spurious or harmonic responses.

This problem is prevalent in most of the previously mentioned designs, wherever the bandpass and bandstop functions are not harmonically related.

The introduction of shunt shorted stubs has been used to improve the lower frequency cutoff rate in an ultra-wideband bandpass filter [19]. A high-impedance line loaded with radial lines forms a low-pass filter with ultra-wide stopband [20], which is transformed to bandpass filter with high upper rejection by the addition of two shorted stubs. A wide passband response has been split in two [21], and the upper suppressed. In spite of a secondary transmission path, only a modest level of suppression is realized. A cascade of sections consisting of unit elements and Shunt-connected open- and shorted stubs, with extended lengths [22] has good passband performance, but spurious spikes degrade the stopband.

In this paper, the design presented is based on a suitable ultra-wideband bandstop filter, to which transmission zeros are introduced at the origin by the introduction of shunt shorted stubs at specific nodes. The introduction of the shunt shorted stubs forms a bandpass response separated from its upper harmonic by an ultra-wide stopband. All elements resonate at the same fundamental frequency, or sub-multiples of it. Two examples are included; one is based on a simple 5<sup>th</sup> order Chebyshev bandstop design, while the other is based on a pseudo-elliptic ultra wideband bandstop filter [23]. A prototype filter, based on the latter, is constructed and evaluated.

## II. DESIGN APPROACH

An ultra-wideband (UWB) bandstop (BS) filter is modified by the introduction of transmission zeros at the origin to modify the lowpass band of the UWB-BS filter to a bandpass response. The resultant network is termed a composite filter. The width of the stopband between the lower passband and the first harmonic passband,  $B_S$ , is determined by the stopband-width of the BS filter. This filter has a centre frequency  $f_{S0}$ . The BS filter is changed into the composite filter by the introduction of shunt shorted stubs (SSSs). These SSSs introduce transmission zeros at the origin, and thus modify the lowpass band of the BS filter into a bandpass

Submitted: 11 August 2017

J.A.G. Malherbe is with the Department of Electrical, Electronic and Computer Engineering, University of Pretoria, Pretoria 2000, South Africa. (e-mail: jagm@up.ac.za)

response. This procedure is shown schematically in Fig. 1 in the frequency domain:

- 1) Fig. 1(a) shows  $S_{11-BS}$  and  $S_{21-BS}$  for the UWB-BS filter; the stop-band is  $B_S = f_H - f_U$ . The centre frequency of this filter lies at  $f_{S0}$ , and all elements are of a commensurate length,  $\lambda_0/4$ , where  $\lambda_0$  corresponds to the stopband centre frequency  $f_{S0}$ .
- 2) Physically, the UWB-BS filter will consist of a cascade of unit elements and shunt open circuited stubs.
- 3) Fig. 1(a) also shows the transmission response,  $S_{21-SSS}$ , of a simple shunt shorted stub (SSS) of length  $\lambda_0/2$ , and impedance  $Z_{0S} = 150 \Omega$  connected to a  $50 \Omega$  line. The connection of the SSSs to the bandstop filter will be described in the examples.

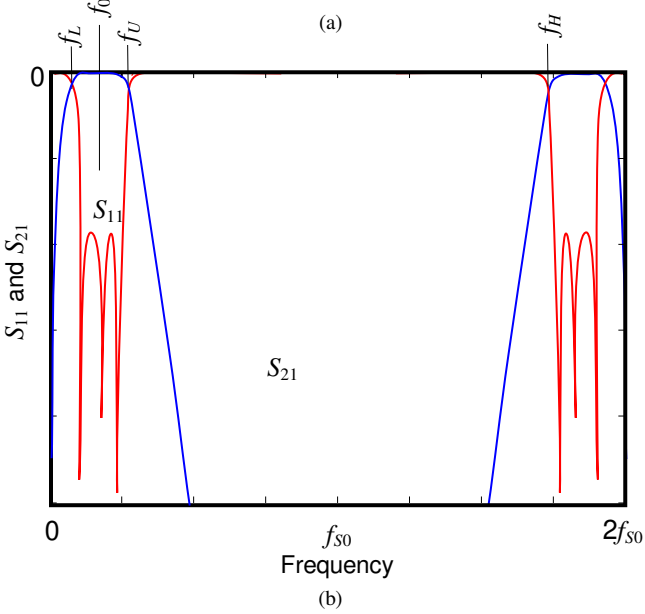
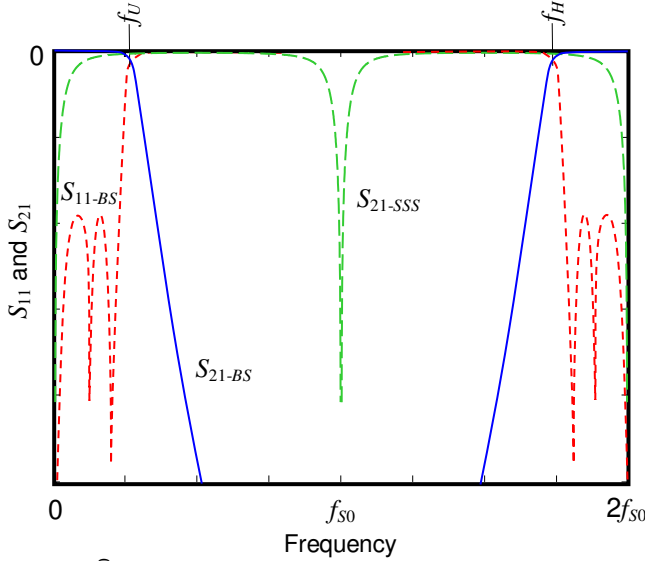


Fig. 1. (a) Schematic Frequency response of UWB bandpass filter,  $S_{11-BS}$  and  $S_{21-BS}$ , and transmission response of SSS,  $S_{21-SSS}$ . (b) Schematic Frequency response of composite filter.

- 4) Connection of the SSS causes transmission zeros at  $f = 0$ ,  $f_{S0}$ , and  $2f_{S0}$ . The passbands that are created in this way

- are shown for the composite filter in Fig. 1(b). The lower passband lies at  $f_L \leq f \leq f_U$ , with a centre frequency of  $f_0$  while the upper passband lies above  $f_H$ . (The latter is not really of any concern.)
- 5) The upper cutoff frequency of the passband,  $f_U$ , coincides for design purposes with the lower cutoff frequency of the bandstop filter; similarly, the lower cutoff frequency of the upper passband coincides with the upper cutoff frequency of the bandstop filter,  $f_H$ .
- 6) The bandwidth of the BSF is therefore determined by  $f_H$  and  $f_L$ ; the centre frequency  $f_{S0} = \frac{1}{2}(f_H - f_L)$ .
- 7) The rate of cutoff of the passband at  $f_U$  is determined to a large extent by the rate of cutoff of the wideband bandstop design, due to the flat passband response of the SSSs. This remains true for high values of SSS impedance.
- 8) The rate of cutoff at  $f_L$  is a function of the length  $N\lambda_0/4$  and  $Z_{0S}$  of the individual stubs employed to create the transmission zeros at the origin. In practice, only values of  $N = 1, 2$  are realistic. For  $N = 1$ , zeros are only formed at 0 and  $2f_{S0}$ .
- 9) The ripple level of the passband of the UWB-BS filter determines the ripple level of the passband of the composite filter. This is independent of the order of filter chosen for the UWB-BS filter. The passband ripple is adjusted by means of the input/output sections to be the same as that of the UWB-BS filter. (See examples in sections III and IV.)
- 10) Note that at  $f_L, f_U$ , and  $f_H$  are  $-3$  dB frequencies.

### III. CHEBYSHEV DESIGN

The design procedure is illustrated by means of a filter with the following specifications:

- Stopband-width  $B_S = f_H/f_U > 5.5$ ,
- Passband-width  $B_P = 100\%$ ,
- Passband Ripple 0.1 dB,
- Cutoff rate: 5<sup>th</sup> order Chebyshev.

A simple 5<sup>th</sup> order Chebyshev prototype with passband ripple of 0.1 dB is used as the wideband bandstop filter. The lumped element prototype is converted to a transmission line network through Richards' transform [24] and impedance scaled to  $50 \Omega$ . The network is frequency scaled to a cutoff frequency of  $\Omega_C = 0.5$  [25], to give a stopbandwidth of  $B_S = 141\%$ . Unit elements are next transformed over the distributed elements by Kuroda's transform [25], to obtain the wideband bandstop filter shown schematically in Fig. 2; element values are given in Table I.  $Z_{U12} - Z_{U45}$  are unit elements, and  $Z_1 - Z_5$  are open circuited stubs.

TABLE I  
ELEMENT VALUES FOR CHEBYSHEV FILTER

Unit Element Impedance ( $\Omega$ )				
$Z_{U12}$	$Z_{U23}$	$Z_{U34}$	$Z_{U45}$	
84.891	152.30	152.30	84.89	
Stub Impedance ( $\Omega$ )				
$Z_1$	$Z_2$	$Z_3$	$Z_4$	$Z_5$
121.7	16.86	12.66	16.86	121.7

In order to realize the passband, three shunt shorted stubs,  $Z_{S1}$ ,  $Z_{S2}$ , and  $Z_{S3}$ , are now connected to this filter, as shown in Fig. 3.

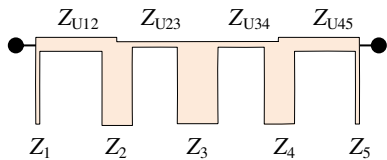


Fig. 2. 5th order Chebyshev wideband bandstop filter

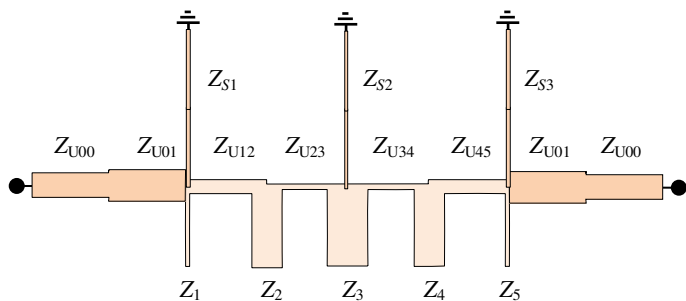


Fig. 3. Connection of SSSs to 5<sup>th</sup> order Chebyshev filter.

The values of the SSSs are determined through iteration by trial and error. This is very readily achieved, as only two variables need to be chosen. Typically, starting values for  $Z_{S1} = Z_{S2} = Z_{S3} = 100 \Omega$  are chosen; because of the symmetry,  $Z_{S1} = Z_{S3}$ . A few iterations yield  $Z_{S1} = Z_{S3} = 110 \Omega$ , and  $Z_{S2} = 140 \Omega$ , for  $B_p \approx 100\%$ . Each SSS has a total length of  $\lambda_0/2$ . The frequency response of the composite filter is compared to that of the Chebyshev prototype in Fig. 4.

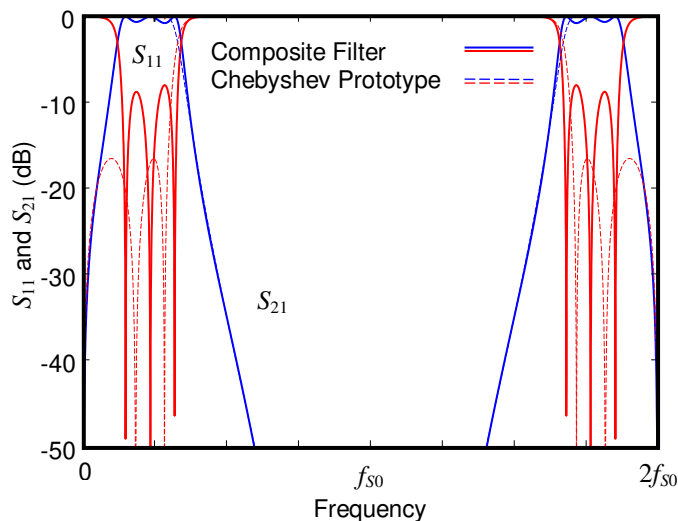


Fig. 4. Frequency response of Chebyshev prototype with three SSSs, compared to the prototype.

However, the return loss of the passband is very poor at this stage; this is corrected by means of the matching unit elements  $Z_{U00}$  and  $Z_{U01}$ . These unit elements are adjusted alternately, until the desired passband return loss is obtained. Slight adjustment of the SSS impedance values might be necessary if return loss ripples of equal level are desired. Final values are shown in Table II.

Unit Elements ( $\Omega$ )		Stubs ( $\Omega$ )	
$Z_{U00}$	$Z_{U01}$	$Z_{S1}, Z_{S3}$	$Z_{S2}$
40.4	40.0	110.0	120.0

The final frequency response of the composite filter is shown in Fig. 5. There has been a slight shift in the upper cutoff frequency of the passband, but this presents no problem, as the SSSs are employed to obtain the desired passband width. The deviation from the Chebyshev response at the upper cutoff frequency  $f_U$  is due to the reactive contribution of the SSSs. The cutoff rate is slightly increased, due to the additional transmission zeros introduced at  $f_{S0}$ .

The centre frequency of the passband,  $f_0 = 0.231f_{S0}$ , and the band edges of the passband lie at  $f_L = 0.498f_0$  and  $f_U = 1.507f_0$ ; the bandwidth,  $B_p = 100.9\%$ .

A conventional bandpass filter would have had harmonic responses at  $0.693f_{S0}$ ,  $1.155f_{S0}$ ,  $1.617f_{S0}$ , while the composite filter has a first harmonic response at  $1.769f_{S0}$ . The ratio between the band edge frequencies of the primary and harmonic responses,  $f_H/f_U = 5.66$ , which equates to the suppression of approximately  $2\frac{1}{2}$  harmonic responses.

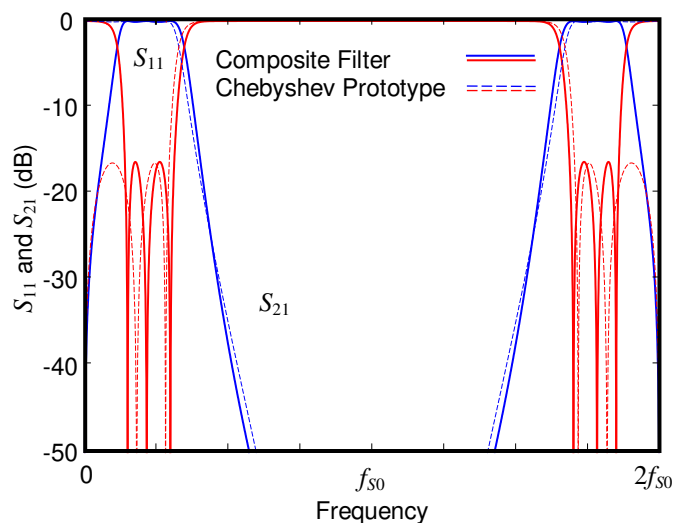


Fig. 5. Frequency response of composite filter after passband match.

#### IV. PSEUDO-ELLIPTIC DESIGN

The second example is based on the application of an UWB-BS filter that was previously described [23], and is a planar structure with  $A_{min} = -30$  dB,  $A_{max} = -17.6$  dB, and bandwidth of 146%. The element values for the filter are given in Table III, [23, Table I]<sup>1</sup> and the unmodified response of the structure is shown in Fig. 6. (The performance is almost identical to that of a fifth order Cauer filter, C0515,  $\Theta = 58^\circ$ , with maximum passband ripple of  $-16.6$  dB and minimum stopband ripple level of  $-29.6$  dB, and exhibits the same very high cutoff rate.)

<sup>1</sup> Table III and Fig. 6 are with permission © EuMA (European Microwave Association) from [23].

TABLE III  
ELEMENT VALUES FOR UWB BANDSTOP FILTER  
(Adapted from [23, Table I]<sup>1</sup>)

Unit Element Impedance ( $\Omega$ )			
$Z_{U01}$	$Z_{U12}$	$Z_{U23}$	$Z_{U34}$
56.0	177.0	165.0	47.0
Stub Impedance ( $\Omega$ )			
$Z_1$	$Z_2$	$Z_3$	
$Z_{11}$	42.5	$Z_{31}$	101.3
$Z_{12}$	69.9	$Z_{32}$	124.5
$Z_{13}$	94.5	$Z_{33}$	83.0
Filter Performance (dB)			
Minimum Stopband	$A_{\min}$		-30
Maximum Passband	$A_{\max}$		-17.6

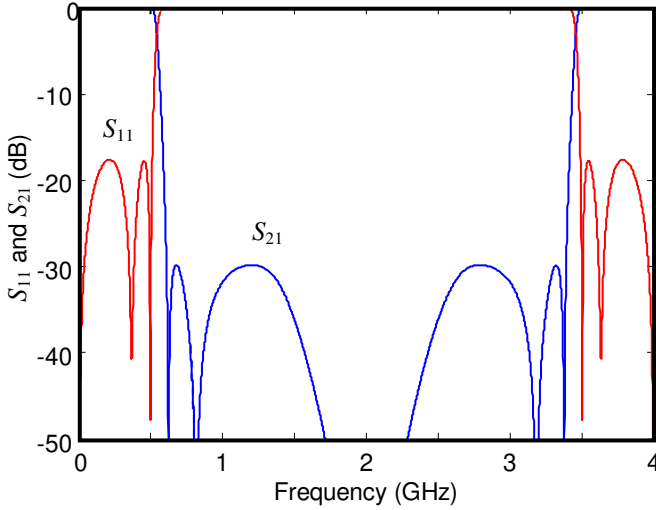


Fig. 6. Calculated response of UWB bandstop filter [23]<sup>1</sup>.

Fig. 7 shows the structure of the composite filter constructed of the UWB-BS filter and two SSSs,  $Z_{S1}$  and  $Z_{S3}$ , each of length  $\lambda_0/2$ .

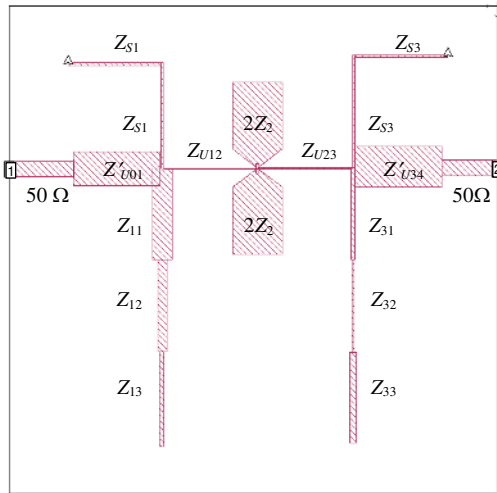


Fig. 7. Structure and SONNET layout of pseudo-elliptic composite filter.

The SSSs were chosen to give a pass bandwidth of approximately 100%, and are each shown as two sections of transmission line of  $\lambda_0/4$  of the same impedance. In this instance, only two SSSs are introduced, because of the very low impedance of the centre stub of the filter. It was necessary to split the centre stub into two parallel stubs, leaving no space for the connection of a centre SSS.

The introduction of the SSSs once again has a substantial effect on the overall impedance level of the structure. However, the prototype UWB filter has two terminal unit elements,  $Z_{U01}$  and  $Z_{U34}$ , and they are adjusted to give a good passband match. The values of  $Z'_{U01}$ ,  $Z'_{U34}$ ,  $Z_{S1}$  and  $Z_{S3}$  are given in Table IV.

TABLE IV  
MODIFICATION OF UWB FILTER

Unit Elements ( $\Omega$ )		Stubs ( $\Omega$ )	
$Z'_{U01}$	$Z'_{U34}$	$Z_{S1}$	$Z_{S3}$
26	24	120	130

No other modifications are made to the bandstop filter. The filter is designed to have a center frequency of  $f_{S0} = 2$  GHz. The passband center frequency is  $f_0 = 352.5$  MHz, and the passband edges lie at  $f_L = 173.0$  MHz and  $f_U = 532.0$  MHz. The bandwidth  $B = 101.8\%$ . The calculated response for the composite filter is compared to a full-wave analysis in Fig. 8. The ratio between the band edge frequencies of the primary and harmonic responses,  $f_H/f_U = 6.52$ .

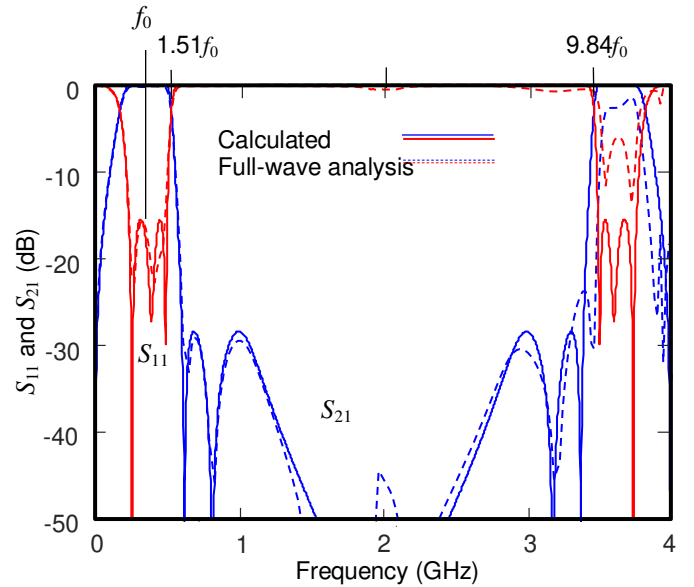


Fig. 8. Calculated response for wideband bandpass composite filter with wide stopband compared to full-wave performance.

Conventional planar Cauer filters based on lumped element prototypes and Kuroda-Levy transforms are not realizable for ultra-wide bandwidths, as some negative impedances result [23].

In practice it was found that little was to be gained with more than three SSSs. Physical restrictions as well as reactive interaction would prevent the addition of more than one SSS

per node. Stubs of commensurate length can be added at one node; they then simply become parallel impedance stubs. All element lengths in both structures are either  $\lambda_0/4$ ,  $\lambda_0/2$  or  $3\lambda_0/4$  at the centre frequency  $f_{S0}$ , and may be stepped or uniform sections. Open circuit stubs of such lengths create transmission zeros at  $f_{S0}$ ;  $\{0.5f_{S0} \pm \Delta f, 1.5f_{S0} \mp \Delta f\}$ ;  $\{0.333f_{S0} \pm \Delta f, f_{S0}, 1.667f_{S0} \mp \Delta f\}$ , respectively, where  $\Delta f$  is determined by the relative impedance values in the case of stepped impedance open circuit stubs [23]. In any event, these zeros always lie inside the bandstop filter stopband, and depending on the zero placement, will create Cauer-like equiripples in the stopband.

## V PHYSICAL STRUCTURE AND MEASUREMENTS

A prototype was constructed on RT Duroid 5880 with dielectric constant  $\epsilon_r = 2.2$  and dielectric thickness 1.575 mm. The etch layout of the filter is shown in Fig. 7. (Note that, with the exception of the unit elements  $Z'_{U01}$ ,  $Z'_{U34}$ , and the stubs  $Z_{S1}$  and  $Z_{S3}$ , the layout is identical to that of [23].)

The dimensions of the elements are given in Table V. The overall size of the filter measures 150 x 150 mm, while the active region of the filter is 110 x 120 mm.

TABLE V  
ELEMENT VALUES AND DIMENSIONS

Element	Impedance $\Omega$	Width mm	Length mm
$Z'_{U01}$	26.0	11.6	26.6
$Z_{U12}$	177.0	0.25	28.9
$Z_{U23}$	165.0	0.33	28.9
$Z'_{U34}$	24.0	12.8	26.5
$Z_{11}$	42.5	6.0	27.1
$Z_{12}$	69.9	2.8	27.8
$Z_{13}$	94.5	1.5	28.2
$2Z_2$	20.8	15.3	26.3
$Z_{31}$	101.3	1.3	28.3
$Z_{32}$	124.5	0.80	28.5
$Z_{33}$	83.0	2.0	28.0
$Z_{S1}$	120	0.9	56.9
$Z_{S3}$	130	0.7	57.1

While the fullwave analysis was performed on the layout as shown in Fig. 7, the physically constructed filter was a modification of the structure of [23], by adding the unit elements  $Z'_{U01}$  and  $Z'_{U34}$  as adhesive-backed copper foil soldered to the original circuit of [23].  $Z_{S1}$  and  $Z_{S3}$  were attached in the same way. Where the one half of each of the latter were bent through  $90^\circ$  in the fullwave analysis, the stubs in the physical circuit were routed to the edge of the board, and earthed with copper strips; a photograph of the filter is shown in Fig. 9.

The measured transmission and reflection performance is compared to the theoretically calculated values in Fig. 10.

The measured performance deviates from the calculated response in a number of ways. Both the maximum return loss in the passband and the minimum insertion loss in the stopband differ from the calculated values, but the passband and stopband ripples are nominally in the same positions, and the differences are of acceptable magnitude.

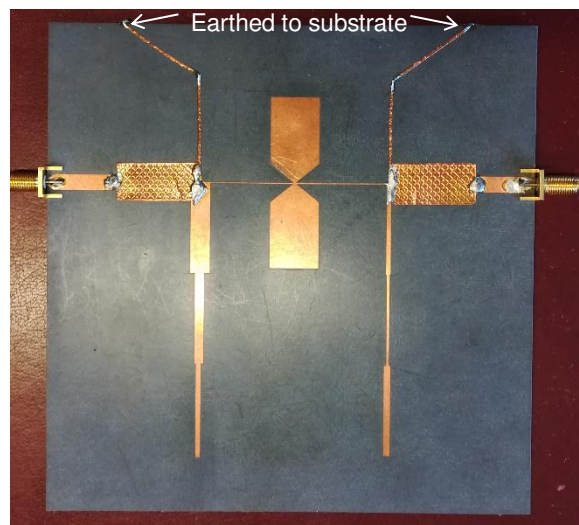


Fig. 9. Photograph of constructed filter.

The measured values for the upper stopband differ substantially from the calculated performance. The stopband cutoff is very close to the calculated value, but the response of the upper passband deviates substantially. This is due to both dielectric loss, as well as radiation. However, the upper passband is not of any consequence – only the cutoff rate is important.

In the centre of the stopband, between 1.5 and 2.5 GHz, the insertion loss exhibits a number of peaks, one of which is reflected in the insertion loss at 1.95 GHz. These unwanted stopband peaks are caused by the fact that no tuning was done on the filter as manufactured; small deviations from the design stub lengths will cause these effects, a phenomenon that is common to all commensurate transmission line filters.

It is clear that no spurious responses occur between the upper edge of the lower passband and the lower edge of the upper passband.

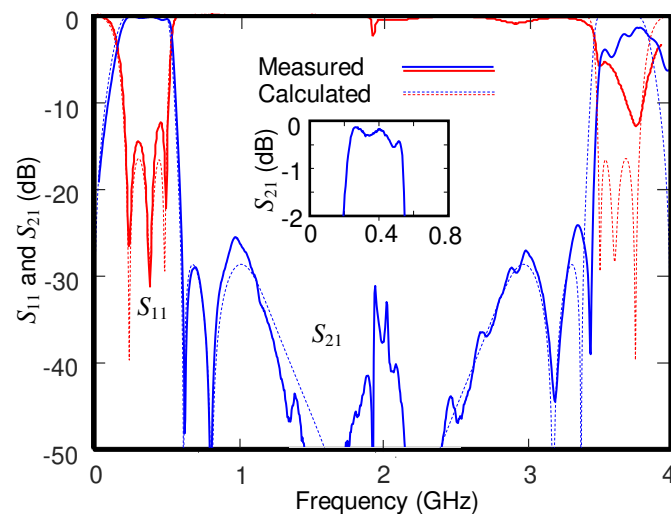


Fig. 10. Comparison of calculated and measured responses for the prototype filter. The inset shows the insertion loss in the passband.

## VI COMPARATIVE PERFORMANCE

The specifications that are relevant to wideband bandpass filters with extended stopbands include passband insertion loss and return loss, and stop-band suppression. The rate of change of  $S_{21}$  at both passband edges is a measure of the selectivity of the passband. The rate at which  $S_{21}$  rises from  $-25$  dB to the  $-3$  dB band-edge,  $f_L$ , is defined as the slope  $S_L$ ; similarly,  $S_U$  is the rate at which  $S_{21}$  drops from  $f_U$  to  $-25$  dB. Then,

$$S_L = 22/(f_L - f_{25}) \text{ dB/MHz},$$

$$S_U = 22/(f_{25} - f_U) \text{ dB/MHz}.$$

The performance of a number of filters referenced in this paper is compared in Table V. The narrowband filter [4] has very high values of  $S_L$  and  $S_U$ ; this is typical of composite filters with narrow passbands. For wider passbands the slopes will typically be less steep, as can be seen from a comparison of filters with passbands around 100%.

However, the filter described in this paper has a substantially higher  $S_U$ , due to the Causer-like cutoff of the bandstop filter on which it is based. The bandwidth ratio of [20] is substantially better than other filters, but probably comes at the cost of the passband width.

TABLE VI  
COMPARISON OF FILTER PERFORMANCE

Ref	$S_L$	$B_p\%$	$S_U$	$B_s/B_p$	$S_{21MAX}$ (Pass) dB	$S_{11MIN}$ (Pass) dB	$S_{21MAX}$ (Stop) dB
[*]	46.6	102	125	7.60	-0.55	-13	-25
[4]	80.6	19.9	140	5.95	>-0.1	-25	-25
[20]	38.9	87	111	15.2	-0.65	-12	-25
[21]	45.6	103	73	1.82	>-0.3	-17	-25
[22]	45.7	104	94	7.37	-0.50	-15	-20

\*This paper.

## VII CONCLUSION

The examples described here both use 5th order UWB-BS filters. In the case of the Chebyshev design, the use of higher order prototypes with wide enough stopband result in structures that are not physically realizable as planar structures, due to extreme impedance levels (both high and low). With reduced stopband-width, higher order designs are realizable, and additional SSSs can be introduced at nodes where convenient. In such instances, additional cascade unit elements might be necessary to achieve a design impedance match.

The proposed composite pseudo-elliptic filter provides a very wide stopband above the wide passband, equivalent to suppression of spurious responses.

The composite filters described here differ from most other designs in that inherently no spurious responses are created in the stopband between passband responses. The occurrence of spurious peaks caused by interaction between stopband elements and passband elements is a serious limitation of most other designs. The spurious responses that do occur in this design are due to the fact that the stub lengths have not been properly tuned to resonate at the same frequencies.

The bandpass response of the filter is not caused by a bandpass filter with conventional harmonic responses, but

rather by the interaction between the highpass SSSs and the cutoff slope of the BSF, so that harmonic responses *per sé* are not relevant. However, approximately four harmonic passbands of a conventional wideband bandpass filter would have been suppressed by the composite filter based on a pseudo-elliptic prototype.

## REFERENCES

- [1] J.-S. Park, J.-S. Yun, and D. Ahn, "A Design of the Novel Coupled-Line Bandpass Filter Using Defected Ground Structure With Wide Stopband Performance," *IEEE Trans. Microw. Theory Techn.*, vol. 50, no. 9, pp. 2037 – 2043, Sept. 2002.
- [2] J.-T. Kuo, W.-H. Hsu, and W.-T. Huang, "Parallel Coupled Microstrip Filters with Suppression of Harmonic Response," *IEEE Microw. Comp. Lett.*, vol. 12, no. 10, pp. 383 – 385, 2002.
- [3] W.M. Fathelbab and M.B. Steer, "Parallel-Coupled Line Filters With Enhanced Stopband Performances," *IEEE Trans. Microw. Theory Techn.*, vol. 53, no.12, pp. 3774 – 3781, Dec. 2005.
- [4] J. Marimuthu, K.S. Bialkowski, and A.M. Abbosh, "Compact Bandpass Filter with Multiple Harmonics Suppression Using Folded Parallel-Coupled Microstrip Lines," in *Asia-Pacific Microw. Conf. (APMC)*, vol. 2, 2015, pp. 1 – 3.
- [5] F.-C. Chen *et al*, "Design of Wide-Stopband Bandpass Filter and Diplexer Using Uniform Impedance Resonators," *IEEE Trans. Microw. Theory Techn.*, vol. 64, no.12, pp. 4192 – 4203, Dec. 2016.
- [6] J. S. Hsieh and C. M. Tsai, "Synthesis of Filters with Stub-Loaded Multimode Resonators," *IEEE Microw. Comp. Lett.*, vol.21, no.10, pp.516 – 518, Oct. 2011.
- [7] L.-Y. Ren and H. He, "Wide stopband bandpass filter based on dual-plane microstrip interdigital DGS slot structure," *Electron. Lett.*, vol. 45, no. 25, pp. 1331 – 1332, 3 Dec. 2009.
- [8] B. Sahu *et al*, "Investigation on Compact Modified Wideband Interdigital Bandpass Filter with Wide Stopband using Spurlines and Defected Ground Structures," *Microw. Opt. Technol. Lett.*, vol. 58, no. 11, pp. 2634 – 2639, Nov. 2016.
- [9] C.-S. Kim *et al*, "A Design of a Ring Bandpass Filters with Wide Rejection Band Using DGS and Spur-line Coupling Structures," in *IEEE MTT-S Microw. Symp. Dig.*, 2005, pp. 2183 – 2186.
- [10] J. García-García *et al*, "Microwave Filters With Improved Stopband Based on Sub-Wavelength Resonators," *IEEE Trans. Microw. Theory Techn.*, vol. 53, no. 6, pp. 1997 – 2006, Jun. 2005.
- [11] F. Huang, "Superconducting Spiral Wide Bandpass Filters With Wide Upper Stopband," *IEEE Trans. Microw. Theory Techn.*, vol. 53, no. 7, pp. 2335 – 2339, Jul. 2005
- [12] C.-H. Chi and C.-Y. Chang, "A Wideband CPS Bandpass Filter with Ultra-wide Upper Stopband Using Stepped-Impedance Rat-Race Hybrid Couplers," in *IEEE MTT-S Microw. Symp. Dig.*, 2007, 735 – 738

- [13] . Watanabe *et al*, “Design of a Microstrip UWB Bandpass Filter Having Sharp [2008-00] Attenuations and Wide Stopbands,” in *China-Japan Joint Microw. Conf.*, 2008, pp. 391 – 395.
- [14] R. Gómez-García *et al*, “Low-Pass and Bandpass Filters with Ultra-Broad Stopband Bandwidth Based on Directional Couplers,” *IEEE Trans. Microw. Theory Techn.*, vol. 61, no. 12, pp. 4365 – 4375, Dec. 2013.
- [15] I. M. Salama, “A New Approach for the Design of Wideband Band-pass Filters with Extended Stop-bands,” in *Texas Wireless and Microw. Circuits Syst. Symp.*, 2013, pp. 1 – 4.
- [16] S. Yang, J. Crutcher, B. Ellis, D. Nesby, and W. Mccaa, “First Harmonic Suppression of a Bandpass Filter with an Optimum Bandstop Filter,” in *2014 IEEE SOUTHEASTCON*.
- [17] C. Song, *et al*, “A Novel Ultra-Wideband Filter With Wider Stopband Employing Multiple-Mode Resonator And Low-Pass Filter,” in *16th Int. Conf. Electron. Packag. Technol. (ICEPT)*, 2015 pp. 546 – 549.
- [18] H.N. Shaman, *et al*, “Compact Ultra-wideband (UWB) Bandpass Filter with Wideband Harmonic Suppression,” in *21st Int. Conf. Microw., Radar and Wireless Commun. (MIKON)*, 2016.
- [19] T. Zhang, *et al*, “A multi-mode resonator-based UWB bandpass filter with wide stopband”, *Int. J. Microw. Wireless Technol.*, vol. 8, no. 7, pp. 1031 – 1035, Nov. 2016.
- [20] J. Xu, Y-X. Ji, W. Wu, and C. Miao, “Design of Miniaturized Microstrip LPF and Wideband BPF With Ultra-Wide Stopband,” *IEEE Microw. Comp. Lett.*, vol. 23, no. 8, pp. 397–399, Nov. 2013.
- [21] S.Y. Shi, W.J. Feng, W.Q. Che, and Q. Xue, “Novel Miniaturization Method for Wideband Filter Design With Enhanced Upper Stopband,” *IEEE Trans. Microw. Theory Techn.*, vol. 61, no. 2, pp. 817–826, Feb. 2013.
- [22] R. Zhang, S. Luo, L. Zhu, and L. Yang, “Synthesis and Design of Miniaturized Wideband Bandpass Filters With Scaled Transmission Line for Spurious-Response Suppression,” *IEEE Trans. Microw. Theory Techn.*, vol. 65, no. 8, pp. 2878–2885, Aug. 2017.
- [23] J.A.G. Malherbe, “Pseudo-Elliptic Function Ultra Wideband Bandstop Filter with Stepped Impedance Stubs”, in *Proc. 44th European Microw. Conf.*, Rome, Italy, Oct. 2014, pp. 536 – 539.
- [24] P.I. Richards, “Resistor-transmission-line circuits,” *Proc. IRE*, vol. 36, pp. 217-220, Feb. 1948.
- [25] J.A.G. Malherbe, *Microwave Transmission Line Filters*, Artech House, Dedham, Mass., 1979.



**Johannes (Jan) A.G. Malherbe** (M’75–SM’77–F’94–LF’09) was born in 1940 in Cape Town, and received the B.Sc., B.Eng. and PhD. degrees from the University of Stellenbosch, and the D.Eng. from the University of Pretoria, South Africa.

He was Associate Professor at the University of Stellenbosch from 1970 to 1980. In 1981 he moved to the University of Pretoria, where he was professor until 1988, and from 1989 to 1999 Dean of Engineering. From 2000 to his retirement in 2005, he was Vice-Principal. He has subsequently been with the Department of Electrical, Electronic and Computer Engineering, University of Pretoria.

He is a Fellow of the SA Academy of Engineering, Fellow of the SAIEE and Member of the SA Academy of Science. He was awarded the Havenga Prize for Engineering by the SA Academy for Science and Art, and is a recipient of the IEEE Third Millennium Medal.